

# Coating tolerant thermography inspection system

Jon R. Lesniak, Daniel J. Bazile, Bradley R. Boyce  
Stress Photonics Inc., 3002 Progress Rd. Madison, WI 53716

## ABSTRACT

Coating Tolerant Thermography's ability to differentiate between chipped paint and structural flaws has clearly been demonstrated. However, the functionality of the final inspection system requires the application of the CTT algorithm to thermal stripes. This paper describes the thermal stripe projector, sensor engines and automatic stripe identification and gradient mapping algorithms required by CTT.

**Keywords:** thermography, NDE, crack, bridge, coating tolerant, Forced Diffusion Thermography

## 1. Introduction

### 1.1. Technology review

Thermal methods correlate structural integrity with thermal diffusivity. If the molecular structure is altered, impairing transfer of forces, then the conduction of heat energy is also impeded<sup>1,2</sup>. Coating Tolerant Thermography projects a pattern of dynamic heat to force conduction across cracks (Fig. 1b) thereby, optimizing the measurable thermal gradient<sup>3,4,5,6</sup>.

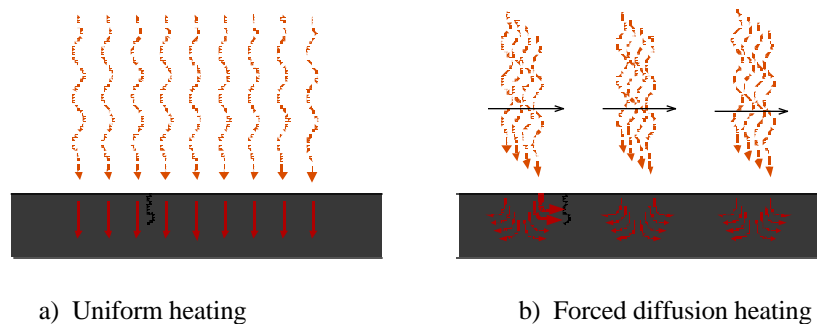


Fig. 1 Thermal methods

Heat travels from “hot” stripe to “cool” stripe as the stripes slowly comb the structure for cracks. The in-plane heat flow is impeded by a structural flaw, such as a crack, creating a gradient in the thermal image, which clearly defines the crack. The fundamental principle behind Coating Tolerant Thermography is that only the thermal spatial derivative of a true structural anomaly will change sign with opposing heat flow. When the heat is flowing from the left, the gradient is positive (as defined) because the heat builds up behind the crack on the left. When heat is flowing from the right, the gradient changes sign becoming negative because now heat builds up behind the crack on the right side. Only a true structural flaw has this characteristic.

A 50 mm x 6.4 mm steel specimen coated with a reflective white paint was prepared with a rusted paint chip near a fatigue crack. Notice the difference in shading of the crack between the first two images (Fig. 2a and Fig. 2b), and the lack of a change in the shading of the paint chip. The emissivity gradient caused by the paint chip is almost completely eliminated from the final data by performing the subtraction of the right and left images. The subtraction process accentuates the crack which impedes the heat flow from both directions.

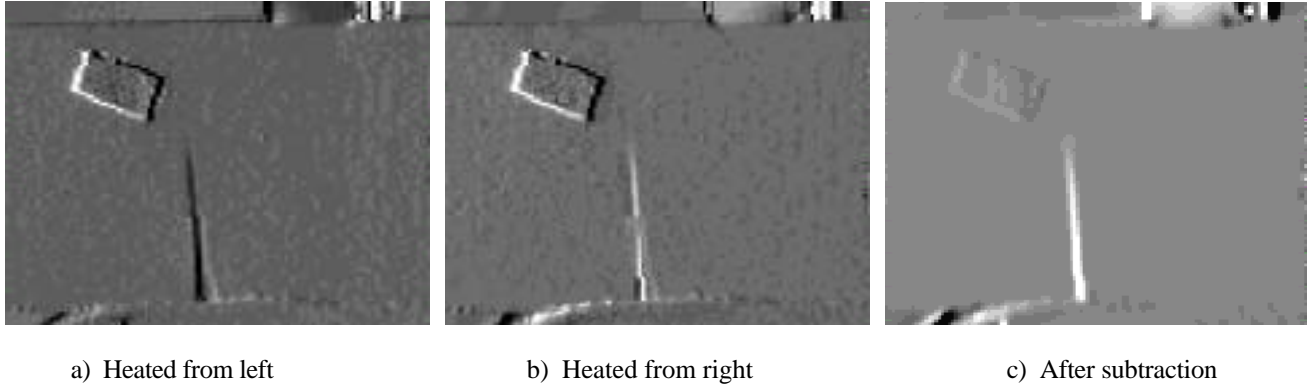


Fig. 2 Coating tolerant Thermography Process

## 1.2 Mathematical derivation

A further understanding of Coating Tolerant Thermography can be gained by mathematical examination of thermal gradient images. Coating Tolerant Thermography measures the thermal distribution before and after heating thereby removing reflections and pre-existing thermal conditions. The difference image,  $I(x,y)$ , is only influenced by a change in the thermal state created by the thermal projection and the emissivity profile of the area,

$$I(x,y) = \phi(x,y) - \epsilon(x,y) \quad (1)$$

where  $\phi(x,y)$  is the photon flux resulting from the added heat or heat lost since the capture of the initial image, and  $\epsilon(x,y)$  is the emissivity profile. Using the product rule, the first spatial derivative with respect to  $x$  normalized by Eq. 1 can be defined

$$\frac{I_x(x,y)}{I(x,y)} = -\frac{\phi_x(x,y)}{\phi(x,y)} + \frac{\epsilon_x(x,y)}{\epsilon(x,y)} \quad (2)$$

which accomplishes a complete separation of emissivity function from the flux function. If the direction of the heat conduction changes, then the  $\phi(x,y)$  (thermal) term changes sign, but the  $\epsilon(x,y)$  (emissivity) term does not. By taking the difference between two images where the direction of the heat conduction is opposite in sign, Coating Tolerant Thermography can discern between real flaws and emissivity variances.

## 2. INSTRUMENTATION

### 2.1. Projector development

The projector utilizes readily available, inexpensive and safe incandescent light sources. The source consumes about 1000W at 120 volts and emits most of its energy in the near infrared below  $3\mu\text{m}$ . The light energy does not significantly conflict with the sensitivity range of typical infrared cameras ( $3\text{-}5\mu\text{m}$  and  $8\text{-}12\mu\text{m}$ ). The projector parses the radiation from the line source into 3 light paths via a gold plated elliptical light separator<sup>7</sup> (Fig. 3). Elliptical reflectors focus energy into two stripes; the radiation emitted in a direction opposite the elliptical reflectors is returned to the elliptical reflectors via cylindrical reflectors. A third stripe is created in the center via direct radiation into a channel augmented by a cylindrical reflector opposite the channel. The three stripes are transferred down reflective guides which not only contain the light in-plane but condition the light in the vertical direction as well.

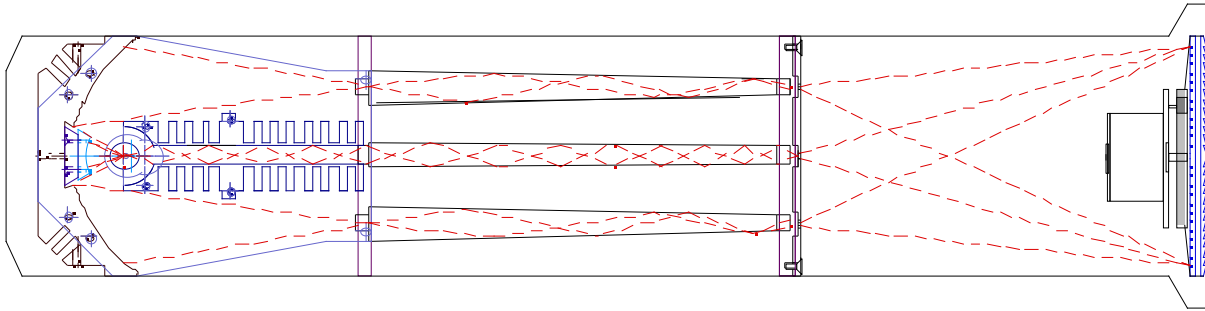
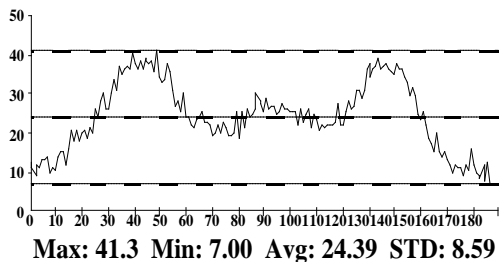


Fig. 3 Top view of projector layout (horizontal light management)

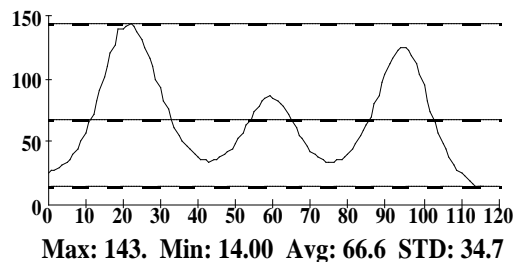
The final portion of the projector is the condenser/projector lens combination, which also gives some flexibility in the adjustment of standoff distance and coverage area. The condenser lenses help direct the rays of light to the projection lens, which then projects the pattern onto the area of interest. The lightweight Fresnel projector lens is translated in order to shift the position of the stripes. All the reflective optics are gold-plated for maximum efficiency. The dimensions of the projection cell are 380 mm x 75 mm x 150 mm. The final system will incorporate several of the 1000 Watt sources so that higher line counts can be achieved. The final configuration will be determined through lab and field testing of actual bridge components.

### 2.2 Infrared cameras

In order to control cost of the final systems, an uncooled bolometer has been chosen as the sensor engine. The uncooled bolometer is very compact and costs as little as 30% of other infrared technologies. There is, however, some compromise in the quality of the data obtainable with the bolometer. Figure 4 compares the ability of a bolometer and a Sterling cooled InSb camera operated at similar sampling times to resolve low magnitude thermal stripes. As can be seen the InSb array camera has 3-4 times the thermal resolution.



a) Bolometer image of hot stripes



b) InSb camera image of hot stripes

Fig. 4 Thermal resolution of bolometer vs. InSb

Because the actual implementation of the gradient filter uses several data points to calculate the spatial derivative, the signal to noise ratio of the gradient calculation is improved (Fig. 5) allowing for good crack detectability (Fig. 6).

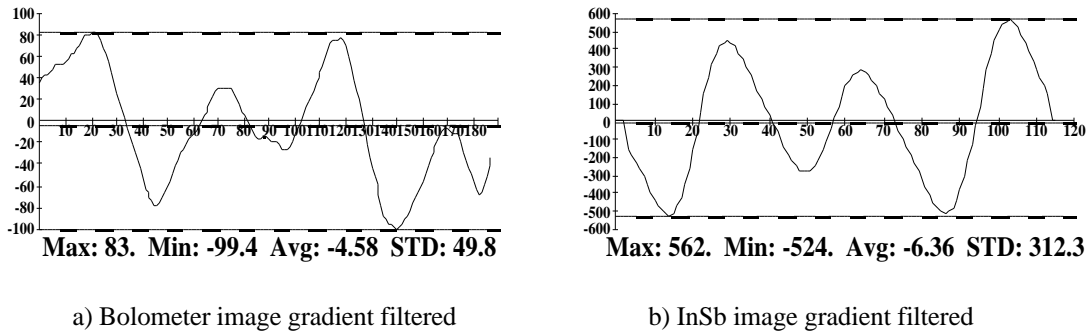


Fig. 5 Thermal resolution considering filter application

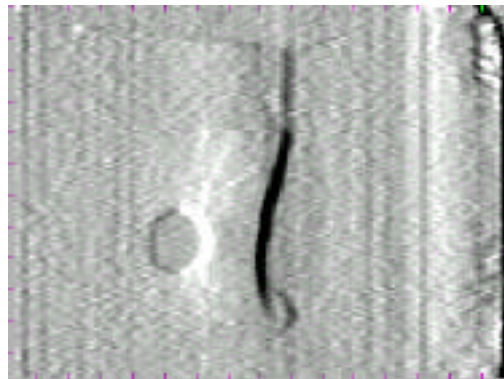


Fig. 6 Gradient Image of crack in steel bridge

Furthermore, unlike passive thermal methods the signal to noise ratio can be improved by increasing the output of the thermal projector. Table 1 compares the attributes of the Sterling cooled InSb camera to the uncooled bolometer.

	ICC Bolometer	SBFP camera
Thermal resolution (1s ave)	50mK	10mK
Spatial Resolution	320 x 240	128 x 128
Wavelength sensitivity	8-12 $\mu$ m	3-5 $\mu$ m
Cost	\$15k	\$50k

Table 1 Comparison of bolometer camera vs. SBFP

### 3.0 Algorithm

Each projected thermal stripe yields a positive and negative gradient zone as heat flows away from the stripe. The stripe is moved through four or more steps to accomplish complete coverage. The final challenge is applying the CTT algorithm to the plethora of thermal images with their respective gradient zones. Because the system is intended to be used on simple but varying geometries the location of the stripes in the image area is not certain. An automatic identification algorithm has been developed. First the algorithm uses a simple kernel filter design to detect positive or negative gradients. The results of the filter are then compared to preset sensitivity limits and converted to logical values -1,0,1 (Fig. 7b). Next, the center of the gradient bands are determined. A smart algorithm is then applied to find a smooth path through the center of the gradient zones (Fig. 7c). Finally, the stripes are expanded to a specified width (Fig. 7d). In this way, positive and negative slope gradients bands are defined for each stripe position.

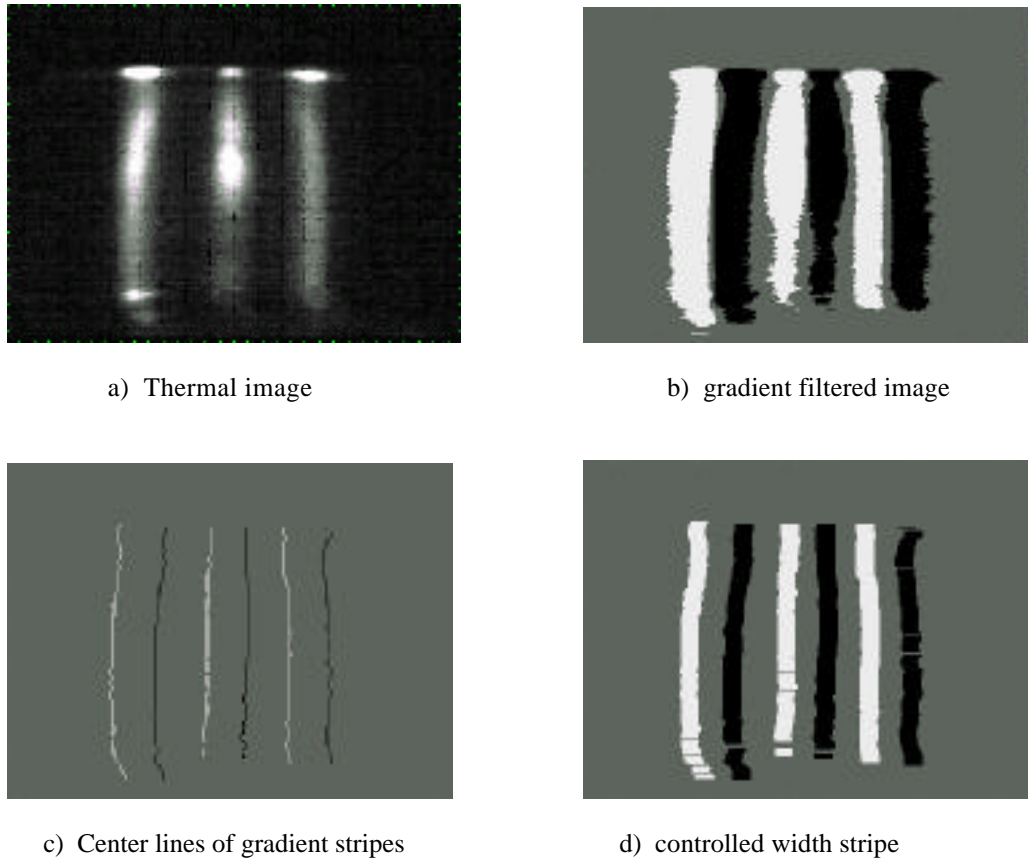


Fig. 7 Gradient mapping algorithm

#### 4.0 CONCLUSIONS

Coating Tolerant Thermography is specifically designed for inspection of large, steel structures that are heavily and nonuniformly coated with paints and perhaps debris. Emissivity variances caused by such nonuniformities are completely eliminated in the final result. There is a clear path to an inexpensive hand held system that will be portable, robust, rapid and widely reproducible. Several issues remain to be resolved including final compilation algorithms.

#### 5.0 ACKNOWLEDGMENTS

Stress Photonics would like to acknowledge the supporters of this research, which included the Federal Highway Administration and the National Aeronautics and Space Administration. There are several individuals without whom this project would not have been possible: Steve Chase of the FHWA, Elliott Cramer of NASA LaRC and Phil Fish of the Wisconsin DOT.

#### 6.0 REFERENCES

1. Cramer, K. E. and Winfree, W. P., "Thermographic imaging of cracks in thin metal sheets," Thermosense XIV, Jan., K. Eklund, Editor, Proc. SPIE Vol. 1682, pp. 162-170, 1992.
2. Osiander, R., Spicer, J. W. M. and Murphy, J. C., "Analysis methods for full-field time-resolved infrared radiometry," Thermosense XVII, April, D. D. Burleigh and J. W. M. Spicer, Editors, Proc. SPIE Vol. 2766, pp. 218-227, 1996.
3. Lesniak, J. R. and Boyce, B. R., "Forced-Diffusion Thermography," Thermosense XVII, Sharon A. Semanovich, Editor, Proc. SPIE Vol. 2473, pp. 179-189, Orlando April 1995.

4. Lesniak, J. R. and Bazile, D. J., "Forced-Diffusion Thermography technique and projector design," Thermosense XVIII, D. Burleigh and J. Spicer, Editors, Proc. SPIE Vol. 2766, pp. 210-217, Orlando, April 1996.
5. Lesniak, J. R., Bazile, D. J. and Zickel, M. J., "Structural Integrity Assessment via Coating Tolerant Forced Diffusion Thermography," ASCE Structures Congress XV, Leon Kempner, Jr. and Colin A Brown, Editors, pp. 924-928, April 13-16, 1997, Portland, OR.
6. Lesniak, J. R., Bazile, D. J. and Zickel, M. J., "Coating tolerant thermography for the detection of cracks in structures," Thermosense XIX, R. N. Wurzbach and D. Burleigh, Editors, Proc. SPIE Vol. 3056 pp.235-241 Orlando, FL, April 1997.
7. Lesniak, J. R., Bazile, D. J. and Zickel, M. J., "Theory and application of coating tolerant thermography," Thermosense XX, John R. Snell, Jr., R. N. Wurzbach, Editors, Proc. SPIE Vol. 3361 pp.325-330, Orlando, FL, April 1998.